_____

# Dense Alumina-Mullite Composite Ceramics from Alumina and Spodumene-albite Feldspar binary mixtures: Processing and Properties

**M. F. Hernández[1,2*)], P. V. López[1], A. Violini[1,2], G. Suárez[1,2], M. S. Conconi[1,2], N. M. Rendtorff[1,2]**

[1]Departamento de química, Facultad de Ciencias Exactas, Universidad Nacional de La Plata, 47 y 115, La Plata 1900 Buenos Aires, Argentina.
[2]CETMIC. Centro de Tecnología de Recursos Minerales y Cerámica (CIC-CONICET La Plata) Cno. Centenario y 506 M.B. Gonnet (1897), Buenos Aires, Argentina.

*Abstract:*
*A processing strategy for obtaining alumina-spodumene ceramics from fine commercial powders is presented. In this work, a spodumene addition to calcined alumina powder was performed and their proportion was explored between 15 and 45 wt%. The industrial spodumene presented secondary phases, mainly albite and quartz. Mechanical properties were evaluated. Although they were lower than those of sintered alumina, based on the achieved values an adequate behavior in structural applications can be assumed, especially taking into account that the better mechanical behavior was coupled with the lower thermal expansion. Relatively low thermal expansion $\approx$ ( 5 x $10^{-1}$ °$C^{-1}$) behaviors were observed in one of the developed materials. Noncrystalline phases containing lithium were detected. We assume that all the lithium oxide incorporated through the spodumene is in the glassy phase after the sintering of the materials. This difference in lithium concentration in the composition of the resulting glass affected the thermal expansion of the developed materials. Particularly with low lithium content (30 wt% of additive) the material performance was enhanced. This, together with the mechanical behavior, encourages structural applications with high thermomechanical solicitations. With the information gathered, a wide range of materials with specific properties can be obtained by modulating the spodumene-alumina proportion only.*
*Keywords: Structural ceramics; Alumina; Spodumene; Processing.*

## 1. Introduction

Composite materials have an important industrial and technological role in advanced ceramics. The manufacturer's capability to design properties and behaviors is enhanced by combining two or more different materials. However, the final properties will not always be the same as those of the pure material; in fact, in several cases the properties are considerably improved. The final properties and behaviors will always be related to the actual microstructural configuration. This relation has to be established for better microstructural design [1-6].

_____

*) **Corresponding author:** florenciahernandez@cetmic.unlp.edu.ar

Alumina and alumina-based composite materials are a family of ceramics whose principal constituent is aluminum oxide ($Al_2O_3$). On a weight basis, these materials have the largest share of the ceramics world market [1, 5, 7] with multiple applications. Alumina presents high refractoriness, that is, high melting point (2050 °C) and retention of structural integrity at a high temperature. In particular, it experiences practically no deformation under compressive loads at temperatures up to 1200 °C [1]. The additives usually employed for sintering alumina are kaolinitic clays, calcium carbonate, talc or feldspars (sodic or potassic) [1]. They undergo different thermal processes that result in the sintering mechanism of the highly refractory alumina powders and might lead to the formation of a glassy liquid phase or new emerging phases such as mullite or cordierite [5, 7].

The mullite (M – $3Al_2O_3.2SiO_2$) ceramics have had and will continue to have a significant role in the development of traditional and advanced ceramics [8-12]. Mullite is the only stable crystalline phase in the aluminosilicate system, under normal atmospheric pressure from room to elevated temperatures. Its chemical composition ranges from $3Al_2O_3$–$2SiO_2$ to approximately $2Al_2O_3$–$SiO_2$. It has received significant attention during the last decades as a potential structural material for high-temperature applications. Mullite-based composite structural ceramics have particularly been developed [1,5,9,13-16].
Several studies and applications of these binary ceramic composites have been developed in the last decades [17-22]. They present good mechanical and thermomechanical properties, and the firing treatments are usually at lower temperatures than in pure alumina structural ceramics [1, 5, 17].

The reaction sintering process has been widely employed for sintering refractory powders. During the thermal treatment, the consolidation process is achieved simultaneously with one or more chemical processes [1, 5, 6, 23-26].

Lithium is found in very low concentration in igneous rocks. The largest concentrations of lithium-containing minerals are found in granitic pegmatite. The most important of these minerals are spodumene ($Li_2O.Al_2O_3.4SiO_2$) and petalite ($Li_2O.Al_2O_3.8SiO_2$). Spodumene has a theoretical $Li_2O$ content of 8.03 %. Due to its high lithium content, spodumene is considered the most important lithium ore mineral. A typical run of mine ore can contain 1-2 % $Li_2O$, while a typical spodumene concentrate suitable for lithium carbonate production contains 6-7 % $Li_2O$ (75-87 % spodumene). Higher grade concentrates with 7.6 % $Li_2O$ and low iron content are used in ceramics and more demanding industries.

A typical pegmatite deposit can contain quartz, sodium-feldspar (albite), spodumene, lepidolite, petalite, lithiophilite, microcline, and variable amounts of muscovite, and other accessory phases such as spessartine, biotite, pollucite, amphibole and other minerals (Fe-Ti oxides, tourmaline, chlorite, apatite) [27, 28].

Spodumene has three crystalline modifications: (i) α-spodumene, which is the naturally-occurring structure and a member of the pyroxene group [29], is a chain silicate with Si in a tetrahedral coordination and Al and Li in a sixfold coordination [30]); (ii) β-spodumene, which is a recrystallized product that forms when α-spodumene is heated at 800–1100 °C and has interlocked five-membered rings of $(Si,Al)O_4$ [30]; and (iii) γ-spodumene, which is a metastable phase that has been observed when α-spodumene is heated at 700–900 °C [31] but converts to β-spodumene as the temperature is raised further.
The α-spodumene phase is known to be refractory and only reacts with chemical agents when the particles are very fine or when the processing is conducted under a very high pressure [32].

During the calcination, α-spodumene, which has a monoclinic crystal structure and specific gravity of 3.15 $g/cm^3$, is transformed into β-spodumene, which are a less densely packed form of the same mineral with a tetragonal crystal structure and specific gravity of 2.40 $g/cm^3$. The transformation leads to a volumetric expansion of around 30 % that gives greater accessibility to external reagents to penetrate the mineral structure [32].

Recently, β-spodumene was studied as structural material [33] employing pure synthetic spodumene. Spodumene is usually used as secondary fluxing in porcelain formulations [34,35]. Also β-spodumene and alumina powders of high purity were synthesized by aqueous sol-gel processing [33]. Recently, cordierite–spodumene composite ceramics haven proposed and studied for solar heat transmission pipeline [36, 37].

However, in the presence of sodium [38] the thermal behavior will differ considerably, the possible eutectic formed in the $Na_2O$-$Li_2O$-$SiO_2$-$Al_2O_3$ systems would occur at lower temperatures and would present lower viscosities [39-42].

The principal objective of the present work is to obtain alumina-mullite composite materials from binary mixtures of alumina and an industrial (unrefined) spodumene powder. This study includes the formulation effect of the sinterability, the developed crystalline phases, microstructure and technological properties of the resultant materials on the reaction sintering framework. This will enlighten the design strategies of the alumina and alumina-mullite structural ceramics with spodumene as sintering aid or secondary raw material. These fine powder mixtures might be understood as a model of the fine matrix ceramic setting of a coarse-based castable or other spodumene-containing ceramic composites.

## 2. Materials and Experimental Procedures
### 2.1. Materials

Commercial starting powders were employed: calcined $Al_2O_3$ (α-alumina, A-16SG – Almatis GmbH, Germany) and a local industrial spodumene [43, 44] (mesh #200). The chemical and mineralogical composition of the employed spodumene is shown in Table I. The calcined alumina presents $Na_2O$ impurities ($\approx 0.07$ wt%) and a $D_{50} \approx 0.4$ μm. The amount of alkali in the spodumene is 7.5 wt%.

**Tab. I** Chemical and mineralogical composition of the industrial spodumene.

| Oxide | wt% |
|---|---|
| $SiO_2$ | 71.3 |
| $Al_2O_3$ | 20.4 |
| $Li_2O$ | 3.0 |
| $Na_2O$ | 3.3 |
| $K_2O$ | 1.2 |
| LOI | 0.5 |
| **Phase** | **wt%** |
| α- Spodumene | 37.3 |
| Quartz | 22.2 |
| Albite | 28.3 |
| Muscovite | 10.3 |
| Kaolinite | 1.9 |
| Cookeite | Traces |

### 2.2. Formulation and processing

Different alumina-spodumene binary mixtures were studied: AS15, AS30 and AS45 with 15, 30 and 45 wt% of spodumene respectively.

An initial mixture was carried out in an alumina ball mill (OABM255), with ethanol for 2 h. The mixed slurry was dried and sieved through a 100-mesh screen. The samples were shaped by uniaxial pressing at 50 MPa. Thus, 20 x 3 x 3 mm prismatic probes were obtained. These probes were fired in an electric furnace with a heating rate of 5 °C/min up to 1400 °C with two-hour soaking and cooling at 10 °C/min down to 300 °C. Maximum temperature was chosen after a dilatometric study, taking into account previous reports [17, 33].

## 2.3. Characterization

The materials obtained after sintering were characterized. Identification and quantification of crystalline phases were carried out by X-ray diffraction (XRD) (Philips 3020 with Cu-kα radiation, Ni filter, at 40 kV-35 mA). The XRD patterns were analyzed with the program FullProf (3.0 version June 2015), which is a multipurpose profile-fitting program, including Rietveld refinement to perform phase quantification [45, 46] and Le Bail approach to quantify glassy/amorphous phases [47, 48].

The apparent density and open porosity were determined by the Archimedes method in water. The microstructural analysis was performed by scanning electron microscopy (SEM) (JEOL, JCM -6000). Two sample preparations were carried out: free fracture analysis and diamond paste polished samples.

The mechanical properties of the obtained materials were evaluated. The flexural strength ($\sigma_f$) and the static elastic modulus ($E_{st}$) were determined by the three-point bending test in a universal testing machine INSTRON 4483. The dynamic elastic modulus ($E_d$) was measured by the impulse excitation technique with a GrindoSonic Mk5 ''Industrial'' model; at least eight samples were evaluated for each material [49]. Vickers hardness ($H_v$) was determined with a 1 kgf load and ten-second dwelling time (Buehler IndentaMet, USA); the average for each material was 10 indentations.

Finally, the thermal expansion coefficients of the obtained materials were determined by optical differential dilatometry with a heating rate of 10 °C/min up to 1000 °C, in air atmosphere, using alumina as reference material (Linseis L74). A theoretical thermal expansion coefficient ($\alpha_{theo}$) was also estimated by a composite law approach from the volume fractions ($V_i$) and the individual thermal expansion coefficients ($\alpha_i$) in order to compare with the experimental results. The thermal expansion coefficients of $Li_2O$-$SiO_2$-$Al_2O_3$ glasses were systematically studied by Shelby [50] and fall within the 4-16 x $10^{-6}$ °C$^{-1}$ range, as a function of the lithium content.

## 3. Results and Discussion
### 3.1. Textural properties, Archimedes immersion test

Table II compares the textural properties (density and porosity) with the initial spodumene content of the developed materials. The obtained materials can be considered dense ones, although some open porosity was observed in the less added sample AS15. There is an important decrease in the apparent density, which is expectable taking into account the lower specific gravity of spodumene, mullite and silica-based glass (the expectable phases); the mineralogical analysis is shown below. Due to the apparent density obtained, this family of structural materials is classified as relatively light materials if compared with other oxide or non-oxide structural ceramics [1, 2].

**Tab. II** Open porosity and apparent density of samples AS15, AS30 and AS45.

|  | **AS15** | **AS30** | **AS45** |
|---|---|---|---|
| **Open porosity (%)** | 4.0 | 0.3 | 0.3 |
| **Apparent density (g/cm$^3$)** | 3.90 | 3.21 | 2.96 |

### 3.2. Developed crystalline and noncrystalline phases
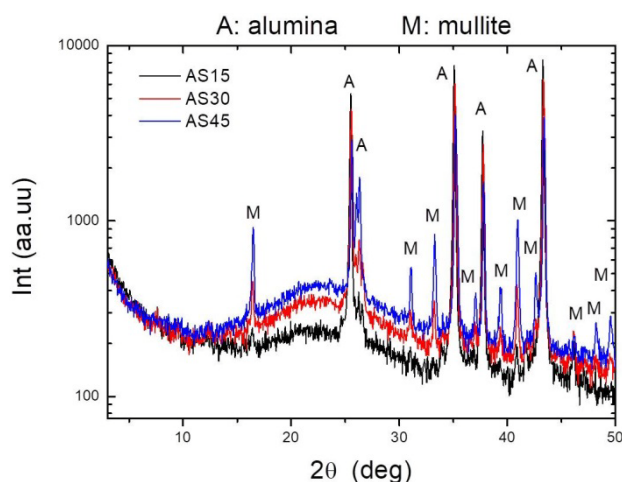


**Fig.1.** XRD patterns of the sintered materials.

Diffraction patterns of the sintered materials are shown in Figure 1. The principal crystalline phases are α-alumina and mullite. No spodumene or lithium based phase was detected. The three studied samples present the typical silica-based amorphous phase band [34, 51]. No crystalline silica ($SiO_2$) phases such as cristobalite or quartz were detected besides glass.

**Tab. III** Phase quantification of sintered materials and PDF cards.

| Sample | Phases | | | |
|---|---|---|---|---|
|  | Alumina | Quartz | Mullite | Glassy phase |
|  | Wt% | | | |
| **PDF card or method** | 01-075-0782 | 01-078-2315 | 00-015-0776 | Le Bail approach [45,51] |
| **AS15** | 93.5 (0.6) | 0.5 (0.1) | 1.3 (0.1) | 4.7 (0.1) * |
| **AS30** | 74.2 (0.5) | 1.0 (0.1) | 7.3 (0.3) | 17.5 (0.2) |
| **AS45** | 50.5 (0.6) |  | 24.3 (0.6) | 25.3 (0.3) |

**\***This determination has high uncertainty for values lower than 10% of glassy phase

It is well known that the vast majority of the $Al_2O_3$-$SiO_2$-$RE_2O_3$ systems (RE: metal) are characterized by their glass-forming abilities [52-54]. In this case, both sodium and lithium present high glass-forming ability. No important results were obtained from the phase refinements; cell parameters were within the reported ones for both crystalline phases. Table 3 summarizes the evaluated and quantified phases in each material. As mentioned, the silica-based glass phase was estimated as well. Global estimated standard deviations were derived from the estimated standard deviation on individual scale factors, for the respective phases, excluding other error contributions and are also presented in the Table.

Evidently, the obtained ceramics correspond to alumina materials [1]. The AS15 corresponds to an alumina sample with a small amount of mullite and glass as sintering aid. On the other hand, AS45 corresponds to a composite with alumina and mullite as principal phases. AS30 has intermediate proportions.

## 3.3. Microstructure

The developed microstructure encourages the future structural application of these composite materials. Figure 2 shows SEM images of the AS materials fired at 1400 °C with different spodumene initial proportions. Both free fracture and diamond paste polished samples are shown.
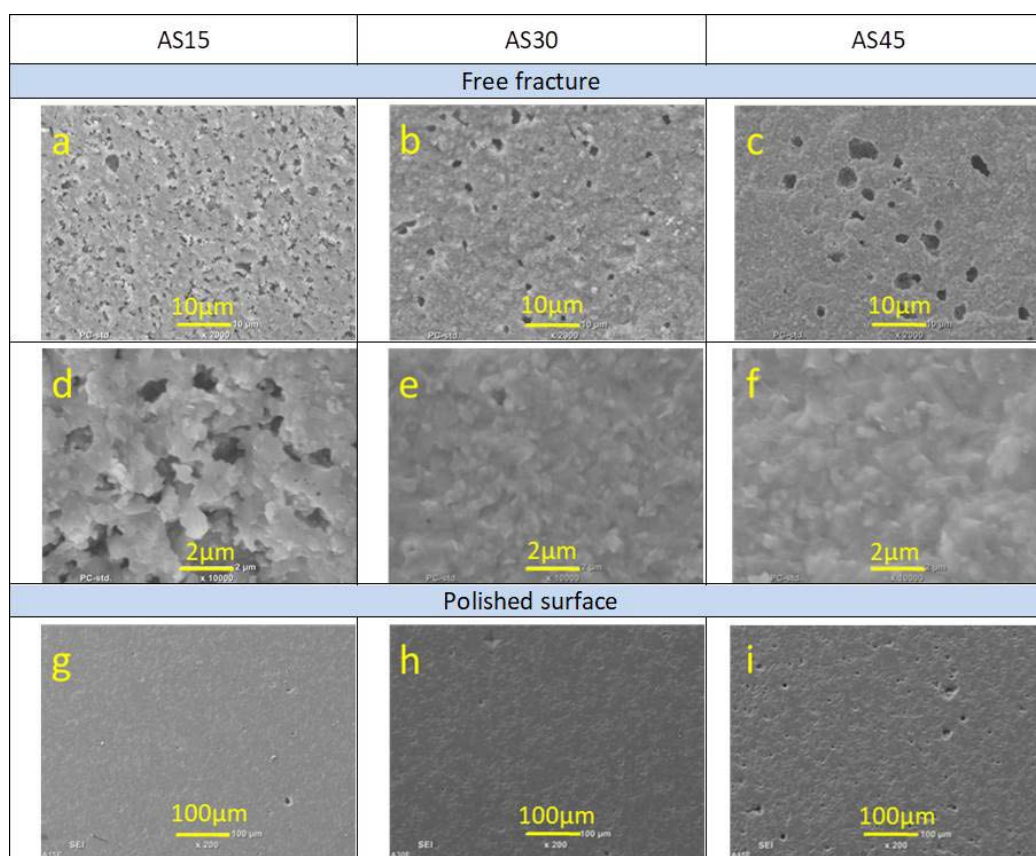


**Fig. 2.** SEM images of the AS15, AS30 and AS 45 samples: a, b, c, d, e and f images correspond to free fracture samples and g, h and i to polished ones.

The homogeneous densification can be observed; however, some macropores ($\approx$ 2-10 μm) corresponding to close porosity can be identified, especially in samples AS30 and AS45. The close porosity evidences a liquid phase sintering mechanism. This might be a consequence of the inefficient green compaction achieved by the uniaxial press; it could be decreased if a better forming technique is implemented. Pores are bigger and less in number as the amount of glass in the materials increases. This is expectable if the glass content is taken into account. Besides, some small pores (below 1 μm) can be observed in AS15, showing that the additive, at this proportion, is not completely effective for sintering the alumina grains.

The composite microstructure consists of a dense distribution of alumina and mullite grains that are angular or subangular and present a medium sphericity. No elongated mullite grains can be observed. Grain sizes are around one micron or below. The mullite distribution is homogeneous. The glass phase imbibes the crystalline alumina and mullite grains.

The Vickers indents on the polished surface of the materials are shown in Figure 3, revealing the homogeneous microstructure as well; the indents are adequate. The relation between the indent size and the microstructure shape is adequate to apply the indentation method; no Palmqvist cracks were observed. Hardness values are listed in Table IV.
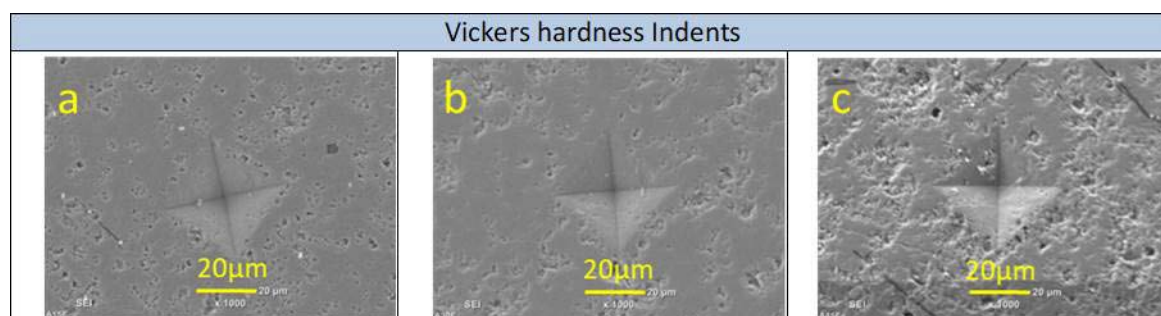


**Fig. 3.**Vickers hardness indent of (a) AS15, (b) AS30 and (c) AS45 samples.

### 3.4. Mechanical behavior

**Tab. IV** Mechanical properties: Flexural strength, elastic modulus and Vickers hardness of sintered materials.

| Mechanical Property | AS15 | AS30 | AS45 |
|---|---|---|---|
| Flexural strength $\sigma_f$ (MPa) | 102 ± 38 | 181 ± 56 | 158 ± 24 |
| Dynamic Young modulus E (GPa) | 9.6 ± 0.4 | 8.5 ± 0.8 | 7.4 ± 1.0 |
| Hv (MPa) | 826 ± 45 | 931 ± 48 | 833 ± 45 |

The mechanical behavior of the sintered materials was studied by three tests: the quasi-static flexural strength, the dynamic elastic modulus by the impulse excitation technique, and Vickers hardness. They provide three mechanical parameters ($\sigma_f$, E and Hv) (Table IV). The achieved results encourage the structural applications of these materials[1, 2, 4]). The evaluated dispersion is within the typical values for structural materials [55].

It is well known that these parameters are strongly related to the microstructure of materials [5, 55] and simultaneously, in multiphase ones, they are correlated with the phase proportions [14, 56-57]. The actual applicability of the structural materials will be achieved only if the mechanical parameters are appropriate. Erosion resistance and other mechanical behaviors are strongly related to these parameters [5]. Sintered alumina can achieve 400-500 MPa flexural strength [1, 54] only if a fully densified microstructure with restricted grain growth develops. This is decreased by the glassy sintering phase and other defects such as porosity.

Although the high specific strength of alumina materials is one of their merits, in some applications lower mechanical performances are adequate. The observed behavior is clearly defined: AS30 presents the highest values for the evaluated mechanical properties ($\sigma_f$ and Hv). It is followed by AS45 and finally, AS15 presents the lowest values. This might be explained by the presence of pores in AS15. Moreover, the increase in the glass content (see Table III) of AS45 explains the decrease in the mechanical behavior at this proportion. Glass presents lower strength in comparison to alumina and mullite [54].

The dynamic stiffness exhibits a different behavior; it gradually decreases with the increase in the initial spodumene content. This is expectable, the glass stiffness ($\approx$70 GPa) is considerably lower than the obtained crystalline phase values: 400 and 220 GPa for alumina and mullite respectively [9, 58-59]. And as shown in Table 3, the amount of glass is proportional to the spodumene proportion.

## 3.5. Thermal expansion behavior of the developed composite materials

The developed materials show a complex thermal expansion behavior, which is expectable taking into account the complex (multiphase) microstructure. They are undoubtedly important for the specific engineering application [1, 5, 54]. Some applications are below 200 °C, others below 400 °C, and other applications involve higher thermal conditions (up to 1000 °C). For severe thermomechanical solicitations, a lower expansion behavior is required [5, 60-61]. The dilatometric curves in the RT-1000°C range are plotted in Figure 4. Estimated thermal expansion values are shown in Table V. The expansion coefficients were calculated from the slope of the fitted linear curve taking into account all the experimental dilatometric data in the specified temperature range. The fitting was good in all the analyzed curves ($R^2$ above 0.98 in all the cases). Besides, a theoretical thermal expansion coefficient ($\alpha_{theo}$) in the RT-1000°C range was calculated assuming the composite law [13]. The volumetric fraction evaluated by the Rietveld refinement and literature thermal expansion values (alumina: 8.0 $10^{-6}$ °$C^{-1}$; mullite: 4.5 $10^{-6}$ °$C^{-1}$; glass: 6.94 $10^{-7}$ °$C^{-1}$ for AS15; 6.18 $10^{-7}$ °$C^{-1}$ for AS30, and 5.5$10^{-7}$ °$C^{-1}$ for AS45) [50, 54] were employed. The predicted expansion coefficients follow the AS45<AS30<AS15 sequence; however, at low temperature the sequence AS30<AS45<AS15 was observed instead.
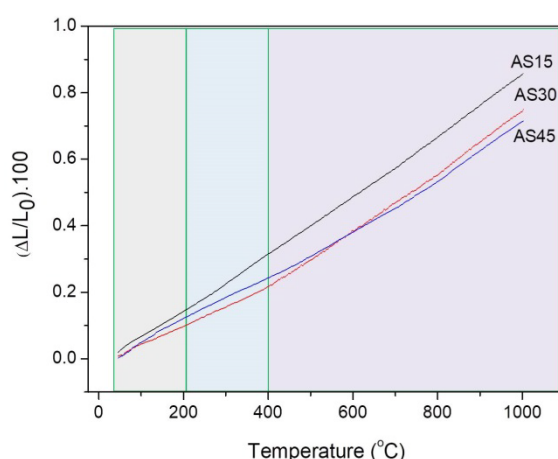


**Fig. 4** Dilatometric curves in the RT-1000 °C range.

The high alumina material (AS15) presents the highest expansion behavior, which is similar to that of alumina polycrystalline ceramics, as expected if the phase proportion is taken into account [1]. On the other hand, for the composites AS30 and AS45 the thermal

expansion coefficients are lower. In fact, below 400 °C, the AS30 material presents 5.73 $10^{-6}$ $°C^{-1}$. This might be advantageous in some severe thermomechanical applications. Remarkably, for this material the experimental value is similar to the theoretical prediction. The AS45 materials present more than 20 wt% of glass phase, which might influence the expansion behavior, especially if the transformation temperature is exceeded. In the same material, at lower temperature the amount of lithium in aluminosilicate glass affects the thermal expansion behavior, and as demonstrated by Shelby et al., if the lithium oxide proportion in the glass is high, the thermal expansion coefficient is comparable to the one of alumina oxide [50]. Finally, the high amount of mullite also lowers the thermal expansion values [10]. All this explains the failure of the composite law.

**Tab. V** Thermal expansion coefficients of sintered materials.

| Temperature range (°C) | Thermal expansion coefficient ($10^{-6}$ $°C^{-1}$) | | |
|---|---|---|---|
| | AS15 | AS30 | AS45 |
| $\alpha_{theo\ (25-1000°C)}$ | 7.09 | 5.82 | 4.64 |
| 50-200 | 7.66 | 5.73 | 7.82 |
| 200-400 | 8.74 | 5.83 | 6.05 |
| 400-1000 | 9.04 | 8.83 | 7.89 |

## 4. Conclusion

- Alumina–mullite composites were successfully obtained from fine commercial powders and characterized. For this purpose, spodumene was added to calcined alumina powder, and their proportion, explored between 15 and 45 wt%, was the principal processing variable. The chosen spodumene presented secondary phases, mainly albite and quartz.
- Developed phases were established, dense ceramics were obtained, and complex microstructures were described. The materials presented a multiphasic interlocked grain microstructure with glass phase as sintering phase from the $Li_2O$-$Na_2O$-$Al_2O_3$-$SiO_2$ system.
- After the thermal treatment, mullite formation was observed. Secondary chemical processes associated with spodumene and albite transformations and fusion were found. New phase development was determined. A sintering liquid mechanism was observed, which enhanced the material sinterization that was also completed.
- Mechanical characterization was evaluated. Although the mechanical properties were lower than those of sintered alumina, based on the achieved values an adequate behavior in structural applications can be assumed, especially taking into account that the better mechanical behavior was coupled with the lower thermal expansion.
- A relatively low thermal expansion ($\approx 5 \times 10^{-1}$ °C) coefficient was observed in one of the developed materials. The lithium concentration in the sintering glass phase affected the expansion behavior. The lithium concentration in the sintering glass phase affected the expansion behavior; with low lithium content (30 wt% of additive) the material performance was enhanced. This, together with the mechanical behavior detected, encourages structural applications with high thermomechanical solicitations.
- With the information gathered, a wide range of materials with specific thermomechanical properties can be obtained by modulating the spodumene-alumina proportion only.

**Acknowledgments**

MFH acknowledges CONICET for the fellowships; this work was partially financed by ANPCyT (PICT-2016-1193) and CONICET (PIO CONICET-UNLA 2016-2018. No. 22420160100023), and UNLP (2015-2018 X-737). MSC is member of the CIC-PBA; MG, GS and NMR are members of the CONICET.

**5. References**

1.  C. Baudín, 2.02 - Processing of Alumina and Corresponding Composites, in: V.K. Sarin (Ed.), Comprehensive Hard Materials, Elsevier, Oxford, 2014: pp. 31–72. doi:10.1016/B978-0-08-096527-7.00021-0.
2.  K. Niihara, New Design Concept of Structural Ceramics, J. Ceram. Soc. Japan. 99 (1991) 974–982. doi:10.2109/jcersj.99.974.
3.  N. M. Rendtorff, S. Gómez, M.R. Gauna, M.S. Conconi, G. Suarez, E.F. Aglietti, Dense mullite-zirconia-zirconium titanate ceramic composites by reaction sintering, Ceramics International. 42 (2016) 1563–1572. doi:10.1016/j.ceramint.2015.09.106.
4.  P.H.C. Camargo, K.G. Satyanarayana, F. Wypych, Nanocomposites: Synthesis, structure, properties and new application opportunities, Materials Research. 12 (2009) 1–39. doi:10.1590/S1516-14392009000100002.
5.  W.E. Lee, R.E. Moore, Evolution of in Situ Refractories in the 20th Century, Journal of the American Ceramic Society. 81 (1998) 1385–1410. doi:10.1111/j.1151-2916.1998.tb02497.x.
6.  G.M. Zeer, E.G. Zelenkova, N.S. Nikolaeva, S.M. Zharkov, A.K. Abkaryan, A.A. Mikheev, Microstructure and phase composition of the two-phase ceramic synthesized from titanium oxide and zinc oxide, Science of Sintering. 50 (2018) 173–181. doi:10.2298/SOS1802173Z.
7.  C. Sadik, I.-E. El Amrani, A. Albizane, Recent advances in silica-alumina refractory: A review, Journal of Asian Ceramic Societies. 2 (2014) 83–96. doi:10.1016/j.jascer.2014.03.001.
8.  W.E. Lee, G.P. Souza, C.J. McConville, T. Tarvornpanich, Y. Iqbal, Mullite formation in clays and clay-derived vitreous ceramics, Journal of the European Ceramic Society. 28 (2008) 465–471. doi:10.1016/j.jeurceramsoc.2007.03.009.
9.  H. Schneider, J. Schreuer, B. Hildmann, Structure and properties of mullite-A review, Journal of the European Ceramic Society. 28 (2008) 329–344. doi:10.1016/j.jeurceramsoc.2007.03.017.
10. R. Torrecillas, J.M. Calderón, J.S. Moya, M.J. Reece, C.K.L. Davies, C. Olagnon, G. Fantozzi, Suitability of mullite for high temperature applications, Journal of the European Ceramic Society. 19 (1999) 2519–2527. doi:10.1016/S0955-2219(99)00116-8.
11. M. Hamidouche, N. Bouaouadja, C. Olagnon, G. Fantozzi, Thermal shock behaviour of mullite ceramic, Ceramics International. 29 (2003) 599–609. doi:10.1016/S0272-8842(02)00207-9.
12. M.F. Serra, M.S. Conconi, M.R. Gauna, G. Suárez, E.F. Aglietti, N.M. Rendtorff, Mullite (3Al2O3·2SiO2) ceramics obtained by reaction sintering of rice husk ash and alumina, phase evolution, sintering and microstructure, Journal of Asian Ceramic Societies. 4 (2016) 61–67. doi:10.1016/j.jascer.2015.11.003.
13. N.M. Rendtorff, S. Gómez, M.R. Gauna, M.S. Conconi, G. Suarez, E.F. Aglietti, Dense mullite-zirconia-zirconium titanate ceramic composites by reaction sintering, Ceramics International. 42 (2016) 1563–1572. doi:10.1016/j.ceramint.2015.09.106.

14. N.M. Rendtorff, L.B. Garrido, E.F. Aglietti, Mechanical and fracture properties of zircon-mullite composites obtained by direct sintering, Ceramics International. 35 (2009) 2907–2913. doi:10.1016/j.ceramint.2009.03.040.

15. N.M. Rendtorff, G. Suárez, Y. Sakka, E.F. Aglietti, Dense mullite zirconia composites obtained from the reaction sintering of milled stoichiometric alumina zircon mixtures by SPS, Ceramics International. 40 (2014) 4461–4470. doi:10.1016/j.ceramint.2013.08.119.

16. N.M. Rendtorff, L.B. Garrido, E.F. Aglietti, Effect of the addition of mullite-zirconia to the thermal shock behavior of zircon materials, Materials Science and Engineering A. 498 (2008) 208–215. doi:10.1016/j.msea.2008.08.036.

17. C. Aksel, The effect of mullite on the mechanical properties and thermal shock behaviour of alumina–mullite refractory materials, Ceramics International. 29 (2003) 183–188. doi:10.1016/S0272-8842(02)00103-7.

18. N. Tamari, I. Kondoh, T. Tanaka, H. Katsuki, Mechanical properties of alumina-mullite whisker composites, Nippon Seramikkusu Kyokai Gakujutsu Ronbunshi/Journal of the Ceramic Society of Japan. 101 (1993) 721–724. doi:10.2109/jcersj.101.721.

19. H.H. Luo, F.C. Zhang, S.G. Roberts, Wear resistance of reaction sintered alumina/mullite composites, Materials Science and Engineering: A. 478 (2008) 270–275. doi:10.1016/j.msea.2007.05.104.

20. F.C. Zhang, H.H. Luo, S.G. Roberts, Mechanical properties and microstructure of $Al_2O_3$/mullite composite, Journal of Materials Science. 42 (2007) 6798–6802. doi:10.1007/s10853-006-1402-z.

21. C. Aksel, Mechanical properties and thermal shock behaviour of alumina–mullite–zirconia and alumina–mullite refractory materials by slip casting, Ceramics International. 29 (2003) 311–316. doi:10.1016/S0272-8842(02)00139-6.

22. C. Aksel, The effect of mullite on the mechanical properties and thermal shock behaviour of alumina–mullite refractory materials, Ceramics International. 29 (2003) 183–188. doi:10.1016/S0272-8842(02)00103-7.

23. Y.-F. Chen, M.-C. Wang, M.-H. Hon, Phase transformation and growth of mullite in kaolin ceramics, Journal of the European Ceramic Society. 24 (2004) 2389–2397. doi:10.1016/S0955-2219(03)00631-9.

24. C.Y. Chen, G.S. Lan, W.H. Tuan, Preparation of mullite by the reaction sintering of kaolinite and alumina, Journal of the European Ceramic Society. 20 (2000) 2519–2525. doi:10.1016/S0955-2219(00)00125-4.

25. J.A. Pask, A.P. Tomsia, Formation of Mullite from Sol-Gel Mixtures and Kaolinite, Journal of the American Ceramic Society. 74 (1991) 2367–2373. doi:10.1111/j.1151-2916.1991.tb06770.x.

26. S. Gómez, G. Suárez, N.M. Rendtorff, E.F. Aglietti, Relation between mechanical and textural properties of dense materials of tetragonal and cubic zirconia, Science of Sintering. 48 (2016) 119–130. doi:10.2298/SOS1601119G.

27. Q. Tian, B. Chen, Y. Chen, L. Ma, X. Shi, Roasting and leaching behavior of spodumene in sulphuric acid process, Xiyou Jinshu/Chinese Journal of Rare Metals. 35 (2011) 118–123. doi:10.3969/j.issn.0258-7076.2011.01.022.

28. O. Peltosaari, P. Tanskanen, E.-P. Heikkinen, T. Fabritius, $\alpha \rightarrow \gamma \rightarrow \beta$-phase transformation of spodumene with hybrid microwave and conventional furnaces, Minerals Engineering. 82 (2015) 54–60. doi:10.1016/j.mineng.2015.04.012.

29. W.A. Deer, R.A. Howie, J. Zussman, An introduction to the rock-forming minerals, 3. edition, The Minerological Society, London, 2013.

30. I.L. Botto, Structural and spectroscopic properties of leached spodumene in the acid roast processing, Materials Chemistry and Physics. 13 (1985) 423–436. doi:10.1016/0254-0584(85)90015-X.

31. N.P. Kotsupalo, L.T. Menzheres, A.D. Ryabtsev, V.V. Boldyrev, Mechanical activation of α-spodumene for further processing into lithium compounds, Theoretical Foundations of Chemical Engineering. 44 (2010) 503–507. doi:10.1134/S0040579510040251.

32. N.K. Salakjani, P. Singh, A.N. Nikoloski, Mineralogical transformations of spodumene concentrate from Greenbushes, Western Australia. Part 1: Conventional heating, Minerals Engineering. 98 (2016) 71–79. doi:10.1016/j.mineng.2016.07.018.

33. M. Awaad, H. Mörtel, S.M. Naga, Densification, mechanical and microstructure properties of β-spodumene - Alumina composites, Journal of Materials Science: Materials in Electronics. 16 (2005) 377–381. doi:10.1007/s10854-005-1149-3.

34. W.M. Carty, U. Senapati, Porcelain-Raw Materials, Processing, Phase Evolution, and Mechanical Behavior, Journal of the American Ceramic Society. 81 (1998) 3–20. doi:10.1111/j.1151-2916.1998.tb02290.x.

35. M.F. Serra, M. Picicco, E. Moyas, G. Suárez, E.F. Aglietti, N.M. Rendtorff, Talc, Spodumene and Calcium Carbonate Effect as Secondary Fluxes in Triaxial Ceramic Properties, Procedia Materials Science. 1 (2012) 397–402. doi:10.1016/j.mspro.2012.06.053.

36. J. Wu, C. Hu, C. Ping, X. Xu, W. Xiang, Preparation and corrosion resistance of cordierite–spodumene composite ceramics using zircon as a modifying agent, Ceramics International. 44 (2018) 19590–19596. doi:10.1016/j.ceramint.2018.07.205.

37. C. Hu, J. Wu, X. Xu, P. Chen, Investigating the effect of andalusite on mechanical strength and thermal shock resistance of cordierite-spodumene composite ceramics, Ceramics International. 44 (2018) 3240–3247. doi:10.1016/j.ceramint.2017.11.096.

38. D. Ataide Salvador, Geometallurgical Variability Study of Spodumene Pegmatite Ores, Central Ostrobothnia - Finland, 2017. http://urn.kb.se/resolve?urn=urn:nbn:se:ltu:diva-66536 (accessed December 17, 2018).

39. G.H. Beall, L.R. Pinckney, Nanophase glass-ceramics, Journal of the American Ceramic Society. 82 (1999) 5–16.

40. E. Antolini, LiCoO2: formation, structure, lithium and oxygen nonstoichiometry, electrochemical behaviour and transport properties, Solid State Ionics. 170 (2004) 159–171. doi:10.1016/j.ssi.2004.04.003.

41. M.J. Toplis, D.B. Dingwell, T. Lenci, Peraluminous viscosity maxima in $Na_2OAl_2O_3SiO_2$ liquids: The role of triclusters in tectosilicate melts, Geochimica et Cosmochimica Acta. 61 (1997) 2605–2612. doi:10.1016/S0016-7037(97)00126-9.

42. G. Urbain, Y. Bottinga, P. Richet, Viscosity of liquid silica, silicates and alumino-silicates, Geochimica et Cosmochimica Acta. 46 (1982) 1061–1072. doi:10.1016/0016-7037(82)90059-X.

43. V.A. Martínez, M.A. Galliski, Geology, mineralogy and geochemistry of las Cuevas pegmatite, San Luis, Revista de La Asociacion Geologica Argentina. 68 (2011) 526–541.

44. M.B. Roquet, Mineralización del depósito pegmatítico María Elena, distrito Conlara, San Luis, Argentina, Serie Correlación Geológica. 28 (2012) 23–38.

45. R.D. Bonetto, P.E. Zalba, M.S. Conconi, M. Manassero, The Rietveld method applied to quantitative phase analysis of minerals containing disordered structures, Revista Geológica de Chile. 30 (2003) 103–115. doi:10.4067/S0716-02082003000100007.

46. H.M. Rietveld, A profile refinement method for nuclear and magnetic structures, J. Appl. Crystallogr. 2 (1969) 65–71.

47. A. Le Bail, Modelling the silica glass structure by the Rietveld method, Journal of Non-Crystalline Solids. 183 (1995) 39–42. doi:10.1016/0022-3093(94)00664-4.

48. Quantitative Analysis of Silicate glass in Ceramic Materials by the Rietveld Method, (n.d.). http://www.ing.unitn.it/~luttero/Publications/EPDIC_V/silicate_glass.html (accessed February 16, 2018).
49. G. Roebben, B. Bollen, A. Brebels, H. Van, D.B. Van, Impulse excitation apparatus to measure resonant frequencies, elastic moduli, and internal friction at room and high temperature, Review of Scientific Instruments. 68 (1997) 4511–4515. doi:10.1063/1.1148422.
50. J.E. Shelby, Viscosity and thermal expansion of lithium aluminosilicate glasses, Journal of Applied Physics. 49 (1978) 5885–5891. doi:10.1063/1.324553.
51. M.S. Conconi, M.R. Gauna, M.F. Serra, G. Suarez, E.F. Aglietti, N.M. Rendtorff, Quantitative firing transformations of a triaxial ceramic by X-ray diffraction methods, Ceramica. 60 (2014) 524–531. doi:10.1590/S0366-69132014000400010.
52. Phys. Rev. Lett. 91, 115505 (2003) - Glass Formation Criterion for Various Glass-Forming Systems, (n.d.). https://journals.aps.org/prl/abstract/10.1103/PhysRevLett.91.115505 (accessed December 20, 2018).
53. T.I. Barry, D. Clinton, L.A. Lay, R.A. Mercer, R.P. Miller, The crystallisation of glasses based on eutectic compositions in the system Li2O-Al2O3-SiO2: Part 1 Lithium metasilicate?□?-spodumene, Journal of Materials Science. 4 (1969) 596–612. doi:10.1007/BF00550116.
54. C.B. Carter, M.G. Norton, Ceramic materials: science and engineering, Second edition, Springer, New York, 2013.
55. A.G. Evans, S.M. Wiederhorn, Proof testing of ceramic materials—an analytical basis for failure prediction, Int J Fract. 10 (1974) 379–392. doi:10.1007/BF00035499.
56. K. Niihara, New design concept of structural ceramics. Ceramic nanocomposites, Nippon Seramikkusu Kyokai Gakujutsu Ronbunshi/Journal of the Ceramic Society of Japan. 99 (1991) 974–982. doi:10.2109/jcersj.99.974.
57. N.M. Rendtorff, L.B. Garrido, E.F. Aglietti, Zirconia toughening of mullite-zirconia-zircon composites obtained by direct sintering, Ceramics International. 36 (2010) 781–788. doi:10.1016/j.ceramint.2009.11.010.
58. H. Ledbetter, S. Kim, D. Balzar, S. Crudele, W. Kriven, Elastic Properties of Mullite, Journal of the American Ceramic Society. 81 (2005) 1025–1028. doi:10.1111/j.1151-2916.1998.tb02441.x.
59. T.F. Krenzel, J. Schreuer, D. Laubner, M. Cichocki, H. Schneider, Thermo-mechanical properties of mullite ceramics: New data, Journal of the American Ceramic Society. 102 (2019) 416–426. doi:10.1111/jace.15925.
60. N. Rendtorff, E. Aglietti, Mechanical and thermal shock behavior of refractory materials for glass feeders, Materials Science and Engineering A. 527 (2010) 3840–3847. doi:10.1016/j.msea.2010.02.053.
61. N.M. Rendtorff, E.F. Aglietti, Thermal Shock Resistance (TSR) and Thermal Fatigue Resistance (TFR) of Refractory Materials. Evaluation Method Based on the Dynamic Elastic Modulus, in: R.B. Hetnarski (Ed.), Encyclopedia of Thermal Stresses, Springer Netherlands, Dordrecht, 2014: pp. 5119–5128. doi:10.1007/978-94-007-2739-7_827.

**Садржај:** *У овом раду представљена је стратегија процесирања алумина-сподумен керамике од финих комерцијалних прахова. Сподумен је додат у калцинисан прах алумине и истраживана је додата количина између 15 и 45 wt%. Индустријски сподумен представља секундарну фазу, углавном албит и кварц. Мерена су механичка својства. Иако су вредности ниже од чисте синтероване алумине, на основу добијених вредности може се предпоставити понашање у структурним применама, посебно ако се узме у обзир да је боље механичко понашање купловано са ниским термалним*

*коефицијентом експанзије. Релативно низак термални коефицијент експанзије (≈5 x 10⁻¹ °C⁻¹) је добијен за произведене материјале. Детктоване су нанокристалне фазе које садрже литијум. Претпостављамо да се сав литијум оксид уградио кроз сподумен у стакластој фази након синтеровања. Разлика у концентрацији литијума у саставу финалног производа утиче на термалну експанзију добијеног материјала. Са малом количином литијума (30 wt% адитива), побољшана су својства материјала. Заједно са механичким својствима, ово представља побољшање код структурних апликација.*
*Са овим прикупљеним подацима, широк ранг материјала са специфичним својствима може бити добијен, само варирајући однос сподумен-алумина.*
***Кључне речи****: структурна керамика, алумина, сподумен, процесирање.*